https://doi.org/10.5194/esurf-2020-3
Preprint. Discussion started: 28 January 2020

Earth Surface Dynamics Discussions

Scale-breaks of suspended sediment rating in large rivers in Germany induced by organic matter

Thomas O. Hoffmann[1], Yannik Baulig[1], Helmut Fischer[1], Jan Blöthe[2]

[1]Bundesanstalt für Gewässerkunde, 56068 Koblenz, Germany
[2]Department of Geography, University of Bonn, 53115 Bonn, Germany

Correspondence to: Thomas O. Hoffmann (thomas.hoffmann@bafg.de)

Abstract. Understanding the dynamics of suspended sediment and associated nutrients is of major relevance for sustainable sediment management aiming to achieve healthy river systems. Sediment rating curves are frequently used to analyze the dynamics of suspended sediments and their potential sources and sinks. Here we are using more than 750 000 measurements of the suspended sediment concentrations (*SSC*) and discharge at 62 gauging stations along 19 waterways in Germany based on the suspended sediment monitoring network of the German water and shipping authority, which started in the 1960ties. Furthermore, we analyse more than 2000 measurements of the loss on ignition (*LOI*) of suspended matter at two stations along the rivers Moselle and Rhine to assess the mineral and organic fraction of the suspended matter. SSC and LOI are analysed in terms of the power law rating to identify discharge depended process regimes of suspended matter.

Our results indicate that for most studied gauging stations, rating coefficients are not constant over the full discharge range, but there is a distinct break in the sediment rating curve, with specific SSC-Q domains above and below this break. The transition of the rating exponent is likely to be a result of a change of controlling factors of the suspended sediment from intrinsic organic matter formation at low flows to extrinsic sediment supply (including mineral and organic fractions) due to hillslope erosion at high flows. Based on these findings we developed a conceptual rating model separating the mineral and organic fraction of the suspended matter in the Germany waterways. This model allows evaluating the sources of the mineral and organic fraction of the suspended matter and gain new insights into the first order control of discharge dynamics of suspended sediments.

1 Introduction

Suspended sediment dominates the sediment transport of almost all lowland rivers of the world (Naden, 2010; Walling, 1996), and represents 90-95% of the global riverine sediment load to the coastal oceans (Syvitski et al., 2005). Silt and clay particles, which comprise the dominant grain size fraction of the suspended sediments, form an important transport medium for nutrients, pollutants and contaminants. Sustainable sediment management aiming to achieve healthy river systems therefore requires a sound understanding of the dynamics of suspended sediment, including its sources and sinks along the riverine flow paths.

https://doi.org/10.5194/esurf-2020-3
Preprint. Discussion started: 28 January 2020


Earth Surface Dynamics Discussions
Open Access
EGU

The dynamics of the suspended sediment is strongly conditioned by sediment characteristics (Owens et al., 2005; van Rijn, 1984; Walling et al., 2000). The size and density of the sediment particles control their propensity to settle within the turbulent flow of the river, counteracting the gravitational settling (Naden, 2010; Partheniades, 2009). The size and density of the fine suspended particles in turn affects their affinity to form aggregates and flocs, due to strong cohesive forces between fine grain particles (Winterwerp and Van Kesteren, 2004). Depending on the sediment sources, suspended particles are either mineral, organic, or a combination of both. Erosion of (organic-rich) topsoil either from hillslopes or floodplains represents an important source of suspended sediment (mainly silt and clay) and supplies large amounts of (allochthones) organic matter with site-characteristic carbon contents (Hoffmann et al., 2009). Sediment supply generated by surface runoff in response to intensive and/or long-lasting rainfall events typically results in increased levels of suspended sediment concentration (SSC) in river channels during higher discharges (e.g. Asselmann, 2000; Gray, 2018).

In addition to the allochthones suspended matter, phytoplankton is an important source of organic suspended matter that is autochthonesly produced within rivers. Especially during summer months, when phytoplankton growth is supported by high water temperatures, the availability of light and high nutrient levels, autochthonous organic matter may dominate the suspended load in many large lowland rivers and those with intense agricultural land use within the river catchment (Cloern, 1999; Hillebrand et al., 2018; Thorp and Delong, 2002). Water flow velocities regulate the water residence times, which in turn affect the time for phytoplankton growth in river systems. Low flow conditions with increased residence times provide favourable conditions for phytoplankton growth or even blooms. In contrast, short residence times can strongly reduce the share of autochthonous biomass in suspended sediments, even if light availability, temperature and nutrient levels are not limited (Fischer, 2015; Quiel et al., 2011).

Besides physical factors controlling the abundance of phytoplankton in river systems, several studies stress the importance of biological controls. For instance, Hardenbicker et al. (2016) suggest that low phytoplankton concentrations in the Rhine are at least partly the result of losses due to grazing by the invasive bivalve mollusk *Corbicula fluminea*, which increased in density since the early 1990ies, while phytoplankton declined during the same time.

Furthermore, predicting the characteristics of the suspended matter is confounded by the heterogeneous and composite structure of flocs and aggregates that are composed of mineral particles as well as living and dead organic matter (Winterwerp et al., 2006). The size of the flocs is a function of the turbulence-induced collision of suspended particles and the cohesive and adhesive forces between the flocs. The latter is strongly controlled by the grain size and the organic matter of the suspended particles. Their size and density, in turn, affects the transport dynamics, with large and dense flocs being predominantly deposited, while flocs with a high organic matter content and a low density are transported over long distances (Winterwerp et al., 2006).

Sediment rating curves are frequently used to analyse the dynamics of suspended sediments and their potential sources and sinks (Asselmann, 2000; Cohn et al., 1992) or to predict suspended sediment yields at ungauged or unfrequently gauged stations (Ferguson, 1986; Horowitz, 2003; Morehead et al., 2003; Syvitski et al., 2000). Rating curves plot SSC as a function of water discharge Q. In many cases, there is a close link between both variables that is mostly described by a power law:

https://doi.org/10.5194/esurf-2020-3
Preprint. Discussion started: 28 January 2020

$$SSC = aQ^b, \quad (1)$$

where a and b are coefficients that depend on the characteristics of the river system. a represents the SSC at unit discharge and the exponent b has been discussed in terms of sediment availability and the erosivity of the stream (Asselmann, 2000; Syvitski et al., 2000). While a varies over several orders of magnitude, depending on the river system characteristics, values of b are typically more confined and range between 0.2 and 2.0 (Syvitski et al., 2000), with lower values in arid environments (i.e. 0.2 to 0.7) and higher values in humid, temperate river systems (i.e. 1.4-2.5, based onReid and Frostick, 1987). However, small changes in the rating exponent b can cause strong changes in SSC, which are in the same order of magnitude as the changes imposed by the (large) variability in a (Syvitski et al., 2000). Using Eq. 1, many studies found a strong negative relationship of a and b (Asselmann, 2000), which is however not a matter of the natural balance between the two rating parameters (as proposed by Syvitski et al., 2000) but an artefact of the statistical analysis as the units of a are depending on b. Warrick (2015) suggests using normalized Q and SSC values to avoid this confusion and provide a statistically sound rating analysis (see also method section).

In most cases, there is a strong scatter of measured values around the regression line from Eq.1. Deviations from the simple power law result from i) hysteresis effects during single flood events (Aich et al., 2014; Zuecco et al., 2016), ii) seasonal changes of water and sediment sources (Asselmann, 2000; Morehead et al., 2003) or iii) long-term trends of changing sediment supply (Warrick, 2015). Event-based deviations are associated to: i) clock-wise hysteresis (i.e. the SSC-peak precedes the Q-peak) with a rapid SSC-increase, due to within-channel mobilization of suspended sediment and subsequent sediment exhaustion, or ii) anti-clock-wise hysteresis (i.e. maximum Q precedes the SSC-peak), due to the long transport distance of sediment sources that are located within the catchment (e.g. arable land on inclined hillslopes with increased soil erosion rates) (Asselmann, 2000). While the general characteristics are well known, it is difficult to predict the rating behaviour as a result of the many confounding processes and linkages.

Most monitoring studies focus on total suspended sediment without fractionation into mineral and organic components. In this respect suspended sediment is equivalent to *seston*, a term used in ecological sciences to describe the total particulate matter including living organisms, organic detritus and inorganic particles (Naden, 2010; Wetzel, 2001). Consequently, most sediment rating studies, which focus on prediction of total SSC levels in river systems based on water discharge or on hysteresis effects of total SSC during single flood events, lump organic and inorganic particles into sediment rating curves. To the authors' knowledge, there is no study that rigorously investigates the influence of the variable mineral and organic fractions in river systems on the rating of sediment.

Here we hypothesize that the mineral and organic fractions of SSC in large German rivers show distinctly different scaling behaviours that are related to independent processes. We test this hypothesis by i) analysing the scaling of total suspended sediment with discharge, before we ii) differentiate between the scaling behaviour of the mineral and organic fractions of the

https://doi.org/10.5194/esurf-2020-3
Preprint. Discussion started: 28 January 2020

suspended sediment against discharge. Furthermore, we develop a conceptional sediment rating model considering the mineral and organic fraction of the suspended sediment transport. To perform this study, we used a rich dataset on suspended sediment in the German waterways and analysed more than 750 000 suspended sediment measurements.

2 Method

2.1 Study sites

In this study we explore daily discharge and suspended sediment measurements at 62 gauging stations along 19 waterways in Germany. The studied rivers comprise the Danube, Rhine, Ems, Weser, Elbe and Oder, including some larger tributaries (Tab. 1 for details and Fig. 1 for location). The gauging stations cover contributing areas from 2,076 to 159,555 km², with a median of 24,424 km². The topography of the river catchments includes the steep high mountain terrain of the European Alps (e.g. Alpine Rhine and Danube) as well as the mountainous regions with various geological settings in Central Europe and the flat terrain of Northern Germany, which is mainly composed of glacial and fluvial Quaternary deposits. The long-term average discharge of all stations ranges from 9 to 2289 m³/s (Tab. 1). The strong control of contributing area on discharge is clearly reflected by the higher (specific) discharges of the rivers Rhine and Danube (Jochenstein station), which are characterized by strong discharge contributions from the Alps (Fig. 2). In contrast, stations in the Elbe and Oder catchments show much lower (specific) discharges at a given catchment area, due to lower rainfalls in the more continental climate, compared to the rivers in West and Central Germany, which are fed by elevated precipitation of the more maritime climate.

2.2 Suspended sediment monitoring in German waterways

Suspended sediment in German waterways has been monitored using daily water samples taken manually by the Federal Waterways and Shipping Administration (Wasserstraßen- und Schifffahrtsverwaltung des Bundes, WSV) at ~70 sampling locations. SSC monitoring started in 1965 resulting in long-term records that cover >30 years for many stations. Here, we selected only those stations from the monitoring network that are not located at artificial channels and that cover periods longer than 10 years (Tab. 1 and Fig. 1), resulting in a total of 62 stations. Data from Maxau station at the river Rhine and from some tributaries haven been formerly presented by Asselmann (2000) and Horowitz (2003) in terms of a rating analysis and by Frings et al. (2014) and Frings e al. (2019) in terms of sediment budget calculations.

At each monitoring site, 5-liter water samples were taken each work day (excluding weekends and legal holidays). During floods, the sampling frequency was increased up to 3 samples per day, unless sampling was stopped due to safety reasons. If more than one sample per day was taken, the SSC was given using the mean of all samples of that day. Water samples were filtered using commercial coffee filters, which were weighed before and after filtering (under constant climatic conditions in the lab with 20°C air temperature und 50% air moisture) to calculate the daily SSC [kg/m³] (Hillebrand 2013). The application of coffee filters is cost-efficient and allows to measure SSC at a large number (i.e. 70 samples per day at the

https://doi.org/10.5194/esurf-2020-3
Preprint. Discussion started: 28 January 2020

national scale) and of sufficient quality. We estimated an average pore diameter of the coffee filters in the range of 0.7 to 1 µm. We therefore miss the smallest particles of the suspended sediments (e.g. fine clays), which represent a minor fraction of the total suspended solids. In general, the suspended sediment mainly contains silt (approx. 75%) and only a small fraction of clay (mostly 10-20 %) and fine sand (mostly below 10%) (for a detailed particle size analysis of the suspended sediment of the river Rhine see Hillebrand and Frings, 2017). Thus fine clay < 1µm are expected to be below 10% of the suspended sediment.

As shown in Tab.1, long-term averages SSC of all stations range between 10.7 and 51.6 mg/l, with an average of 25 mg/l. Long-term discharge weighted averages of SSC are somewhat higher ranging between 11.8 and 84.4 mg/l with a mean of 36 mg/l. In agreement with other national monitoring systems (e.g. Diplas et al., 2008; Habersack and Haimann, 2010; Spreafico et al., 2005; Thollet et al., 2018), SSC values for most stations used in this study include both the mineral and organic material of suspended sediment. Only for two sampling locations, located immediately upstream of the confluence of the rivers Moselle and Rhine in Koblenz, biogeochemical fluxes, namely loss on ignition (*LOI*) and chlorophyll a (*Chla*), are monitored since 1997. At both stations, water samples of 2 to 5 litters were taken at a weekly interval (in contrast to the daily sampling of the stations of the suspended sediment monitoring), resulting in a total of 1033 and 1056 samples from the Rhine and the Moselle, respectively (until end of 2017).

To estimate the *LOI* at both stations, the water samples were filtered using a glass fiber filter with a pore size of about 1 µm (Whatman GF 6, GE Healthcare, Germany). The filter was weighted empty (after heating at 500°C for 1 hour to combust organic remains on the filter) and after filtration. Between filtration and weighting the full filter was dried at 105°C for 24 hours, to obtain the total suspended sediment SSC_{tot} (including the mineral and organic components). The organic component was combusted at 500°C for 1 hour to estimate the LOI of the suspended matter. Based on the *LOI*, we separated the mineral (SSC_{mrl}) and organic (SSC_{org}) fraction of the SSC: $SSC_{org} = LOI \times SSC_{tot}$ and $SSC_{mrl} = (1 - LOI) \times SSC_{tot}$.

For both stations, *Chla* was analysed parallel to the LOI samples. *Chla* was used as a proxy of phytoplankton biomass dynamics in the rivers Rhine and Moselle. *Chla* concentrations were determined using German Standard Methods (DEW, 2007). Briefly, phytoplankton was filtered on glass-fiber filters and pigments were extracted with hot ethanol. Chlorophyll concentrations were determined photometrically (DR 2800, Hach Lange, Germany). *Chla* concentration (given in µg/l) was transferred to living phytoplankton biomass using a C:Chla-ratio of 40 and a particulate organic matter (POM) to particulate organic carbon (POC) ratio of 0.42 (Geider, 1987; Hardenbicker et al., 2014; Hillebrand et al., 2018).

2.3 Rating analysis

To analyse suspended sediment as a function of discharge, we calculate sediment rating curves following Eq. 1. The interpretation of the coefficients a and b in Eq. 1 is impeded by their interdependence as illustrated by units of a that are given by $MT^bL^{-(1+3b)}$ (M, T and L represent dimensions of mass, time and length, respectively; note that the units depend on the exponent b). To avoid this complication and to facilitate the comparison of rating curves between various stations, SSC

https://doi.org/10.5194/esurf-2020-3
Preprint. Discussion started: 28 January 2020

and Q values are normalized using the geometric means (SSC_{GM} and Q_{GM}, respectively) of each station according to Warrick (2015):

$$SSC/SSC_{GM} = a\,(Q/Q_{GM})^b \quad (2)$$

In Eq. (2) a and b are dimensionless. The exponent b can be linked to the reactivity of *SSC* for changing discharge and a represents the normalized *SSC* at Q_{GM}.

For most studied gauging stations, a and b are not constant over the full discharge range, but there is a distinct break in the sediment rating curve, with specific SSC-Q_w domains above and below this break. To estimate the discharge at which this break occurs (Q_{br}), we used three approaches. The first approach is based on the locally weighted scatter smoothing (lowess) regression curve, which was calculated using the gplot-package in R according to Cleveland (1981). We defined Q_{br} to be located at the maximum curvature of the lowess regression curve. In the second approach the lowess curve is split using a sequence of discharges (Q_i) between Q_{min} and Q_{max}. Non-linear least square regression of SSC/SSC_{GM} and Q/Q_{GM} was used for each Q_i and for both subsets (below and above each Q_i). First a and b were estimated for the high-flow subset ($Q > Q_i$). Subsequently, a and b were estimated for the low-flow subset ($Q < Q_i$), while the regression curve was forced to intersect the high-flow regression line at Q_i. For each Q_i the sum of the mean absolute error (MAE) of both regressions was calculated. Q_{br} was set to the Q_i with the minimum of the sum of the mean absolute error (MAE). The third approach is similar to the dual regression of the lowess curve, but uses log-binned median SSC/SSC_{GM}. Therefore, Q values were classified into equally spaced classes at a log-scale. For each class, the median *SSC* was calculated. Subsequently, the median SSC/SSC_{GM} values and the mid-point of each Q-class was used for the dual regression analysis to identify Q_{br} at which the sum of the MAE was minimized.

At extreme discharges, rating relationships tend to be strongly scattered due to the low density of $SSC - Q$ datapairs. To estimate the Q_{br}, we thus excluded measurements with Q smaller than the 1% and larger than the 99% discharge percentile of each station.

After the identification of Q_{br} for each station the coefficients in Eq. 2 and their confidence intervals were estimated using a bootstrapping approach with 1000 replicates. Coefficients for the low flow regime (i.e. subset $Q < Q_{br}$) are denoted by a_l and b_l and for the high flow regime (i.e. subset $Q > Q_{br}$) a_h and b_h. To test for significant differences between scaling exponents for the low-flow and high-flow regimes, we compared the distributions of b_l and b_h using a t-test with a 95% confidence level.

The rating for LOI, SSC_{org} and SSC_{min} of the two stations at the rivers Moselle and Rhine in Koblenz was analysed the same way (similar to Eq. 2) as the SSC at the 62 stations from the suspended sediment monitoring network.

https://doi.org/10.5194/esurf-2020-3
Preprint. Discussion started: 28 January 2020

3 Results

3.1 Rating of the total suspended sediment

For 52 out of 62 stations, $SSC - Q$ rating curves show a distinct break in scaling relation (for examples see Fig. 3) with similar values for Q_{br} estimated from three different approaches (Tab. 2). For the remaining 10 stations, no distinct breakpoint is detectable (Fig. 3). After visual inspection and removal of non-plausible break-points of each station, we calculated the average Q_{br} for each station. In general, breakpoints of the $SSC - Q$ relation range between $0.8 < Q_{br} < 1.9$, and show a clustering around 1 (Fig. 4) (the mean Q_{br} over all stations is 1.2), indicating that the breakpoints of many stations are closely located at the geometric mean discharge.

The rating exponent for the low flow regime (b_l) ranges between -0.75 and 1.15 and for the high flow regime (b_h) between -0.6 and 2.45. In general, the distribution of b_l peaks around 0 (median b_l = 0.14, see Fig. 5), with decreasing SSC as a function of Q (i.e. $b_l < 0$) at 19 stations and increasing SSC at 33 stations. b_h is < 0 at 11 stations and > 0 at 51 stations, with a median b_h = 0.83 (Fig. 5). 23 stations are characterized by strong increases of SSC with Q (i.e. $b_h > 1$).

Fig. 6 shows the spatial distribution of the rating coefficients b_l and b_h. Highest b_h-values (positive rating in the high flow regime) are found in the Rhine and its tributaries, Danube and Upper Weser, while the rivers in northern lowland Germany (mainly the Ems, Elbe and Oder rivers) show low b_h-values. Thus differences between the rivers located in the steeper terrain of S and SW Germany and the flat northern lowland rivers are likely controlled by topography. This control is highlighted in Fig. 7, which plots b_h with respect to the fraction of the contributing catchment area that is steeper than 10% slope gradient. Catchments with a higher fraction of steep slopes are characterized be higher b_h-values. Furthermore, the majority of the stations at the rivers Elbe and Oder, which are characterized by low annual rainfall in the contributing catchment, plot below the regression line. In contrast to b_h, b_l does not show a clear spatial pattern nor any relationship to the fractions of steep catchment areas (Fig. 7).

3.2 Rating of the mineral and organic fraction

Since water sampling at the two stations in Koblenz, which provide information on *LOI* and *Chla*, is based on weekly sampling from 1997-2017, in contrast to the daily sampling of the suspended sediment stations (starting from 1964; Tab. 1), we first checked whether the rating of the total SSC is similar to the results from the other stations along the rivers Rhine and Moselle. Indeed Fig. 8a-d and Tab. 2 show the following similarities: i) rating breaks are located at 0.96 and 0.91 of the normalized discharge (Q/Q_{GM}) for the Rhine and the Moselle, respectively, and ii) the rating exponents b_l (0.29±0.20 for Rhine and -0.03±0.07 for Moselle) and b_h (2.26±0.18 for Rhine and 1.54±0.14 for Moselle) are similar to the other stations along the Rhine and the Moselle. However, the lower number of measurements at the LOI-stations (approx. 1000 at both stations) resulted in a larger uncertainty of the parameter estimation (Δb_l and Δb_h) from the bootstrap regression.

The *LOI*- measurements indicate higher organic matter contents in the Moselle (mean *LOI* = 0.385) compared to the Rhine (mean 0.237). *LOI* negatively correlates with discharge at both stations (Fig. 8e+f). However, the relationship for the

https://doi.org/10.5194/esurf-2020-3
Preprint. Discussion started: 28 January 2020

Moselle is much better constrained. High *LOI* values cluster during the summer months (April – September), while low *LOI* values are more prominent during winter months (Fig. 8e+f and Fig. 9). Based on the bootstrap regression, a single power-law ($LOI = a \times (Q/Q_{GM})^b$) was fitted to the *LOI* data, resulting in rating exponents of -0.51 ± 0.03 and -0.47 ± 0.01, and a-coefficients of 0.202 ± 0.003 and 0.319 ± 0.006 for the Rhine and the Moselle, respectively.

Based on the total *SSC* and *LOI*, the mineral fraction of the suspended sediment ($SSC_{mrl} = (1 - LOI) * SSC_{tot}$) was calculated. SSC_{mrl} increases with discharge for both stations (Fig. 8c+d). Yet the variability for any given discharge is large (ranging approximately an order of magnitude) and increases at lower discharges.

In contrast to the *LOI*, *Chla* does not show significant changes with discharge. Fig. 8g+h shows dominantly low Chla values for the Rhine and Moselle. Increased Chla-values are mainly limited to lower discharges ($Q/Q_{GM} < 1$). A more pronounced seasonal pattern with maximum *Chla* values typically in April for the Rhine and May for the River Mosel is shown in Fig. 8 and 9).

4 Discussion

4.1 Controls on rating behaviour of suspended sediment

The sediment rating concept, which expresses suspended sediment concentration (*SSC*) or suspended sediment load (Q_s) as a function of discharge (Q), is based on the assumption that factors controlling the generation of runoff in the catchment are closely linked with factors controlling the sediment supply to the river channel (Gray, 2018). This is certainly the case if rainfall produces erosive surface runoff, which in turn results in sheet, rill and/or gully erosion (e.g.Poesen, 2018) and is supported by the majority of the rating curves presented in this study: 51 of 62 stations show a clear increasing trend with a positive rating exponent in the high flow regime, which is characterized by the production of surface runoff and strong sediment supply through sheet and rill erosion. A positive rating exponent of the SSC-Q relation is associated with a rating exponent > 1 of the Q_s-Q relation:

$$Q_s = SSC \times Q = (aQ^b) \times Q = aQ^{b+1} \quad (3)$$

This implies that the sediment load increases "faster" than the discharge (e.g. sediment load increases more than twofold if discharge doubles) and that additional sediment sources must be mobilized as discharge increases. Rivers showing rapid increases of SSC are termed "reactive" rivers by Syvitski et al. (2000). The (re-)activation of sediment sources can be mainly explained by the increasing connectivity during rainstorm events that leads to an extension of areas of water-saturated soils, which contribute to surface runoff and discharge (Bracken et al., 2013; Fryirs, 2013). Since topography (esp. hillslope gradient, path lengths and surface roughness) exert a dominant control on hydrological and sediment connectivity (Baartman et al., 2013; Heckmann et al., 2018; Hoffmann, 2015), a strong relationship between the rating exponent and the topographic characteristics of the catchments can be anticipated (Gray, 2018; Syvitski et al., 2000). Our results confirm this expectation (Fig. 7b), showing a clear trend of increasing b_h with increasing ratios of inclined hillslopes (i.e. slope gradients > 10%).

https://doi.org/10.5194/esurf-2020-3
Preprint. Discussion started: 28 January 2020


Earth Surface Dynamics Discussions
Open Access
EGU

Thus high b_h values are observed at gauging stations with discharge contributions from the European Alps (e.g. the Danube below Jochenstein and the Rhine) and from tributaries with mountainous catchment topography (e.g. the Neckar and Moselle catchments). Furthermore, our analysis confirms the results by Asselmann (2000), which were obtained by a limited number of stations, with tributaries showing steeper rating curves than the larger river Rhine. Interestingly, most stations from the Elbe and Oder catchments plot below the regression line in Fig. 7b. This indicates that the Elbe and Oder show lower b_h values for a similar fraction of slopes steeper than 10% compared to the general trend. Assuming a similar topography (as expressed by the fraction of steep slopes), the lower b_h values are mainly explained by climatic differences. The dry continental climate in the Elbe and Oder catchments likely reduces the reactivity of the river systems, requiring larger increases of rain and discharge to increase the specific sediment supply in these basins compared to basins with higher/more frequent precipitation in the western part of Germany.

The break of the rating behaviour, which is observed for 52 of the 62 suspended sediment stations along the German waterways, implies a change of processes and/or factors controlling suspended sediment in river channels at the transition from low to high flow regimes. A similar scale break has been shown along the Rhone river in France by Poulier et al. (2019). Interestingly, the break for most stations present in this study occurs at $Q/Q_{GM} \sim 1.1$. Given the ratio of the geometric mean to the average discharge (Q_{avg}) is close to 0.8 for most stations, the rating break and thus the change of processes or controlling factor occurs most likely close to $\sim 0.9 \times Q_{avg}$.

In contrast to b_h, there is no simple relation of the low-flow rating exponent b_l to the topographic characteristics of the contributing catchment (Fig. 7a). This result is not unexpected, given the fact that hillslopes during low flow conditions do not contribute significantly to discharge and suspended sediment in the river channel, but water mainly results from ground water supply. Thus, the transition from b_l to b_h is likely to be a result of a change of controlling factors of the suspended sediment from intrinsic (within the river system) to extrinsic (outside the river channel but within the catchment) factors.

Many of the tributary waterways of the Rhine, and the Upper Rhine itself, are controlled by barrages to support navigation during low flow and to supply energy. Reservoirs upstream of the barrages act as sediment sinks for cohesive fines during low flow conditions. During high flows, weir shutters are opened to prevent damage of the barrages and to control floods. Significant amounts of fine cohesive sediments can be potentially remobilized during high flows if critical shear stresses at the reservoir bed can exceed shear strength of the cohesive fines. However, in most cases weir shutters are only opened during floods, implying resuspension of cohesive sediments only at discharges much higher than Q_{avg}. Furthermore, preliminary evidences indicate that reservoirs upstream of weirs act as sediment sinks esp. during high flows when large amounts of sediment are transported (Hoffmann et al., 2017). It is therefore unlikely that the prominent break at $Q/Q_{avg} \sim 0.9$ is mainly a function of reservoir management. Furthermore, the rating break is also observed in free-flowing waterways (without barrages), pointing to controlling factors not related to the management of the weirs or reservoirs.

https://doi.org/10.5194/esurf-2020-3
Preprint. Discussion started: 28 January 2020

Therefore, the question remains which factors control the rating exponent at low flows and the transition of the rating behaviour at average discharge? Our data show that the share of the organic suspended matter total SSC may play a crucial role of the SCC-rating at low flows.

4.2 Controls of the mineral vs. organic fraction of the suspended sediment

Here we use *LOI* as a measure of the organic fraction of the total suspended solids. Results from the *LOI* measurements at the two stations in Koblenz show generally higher *LOI* values at the Moselle (where LOI > 0.5 is frequently observed) compared to the Rhine, where *LOI* rarely exceed 0.5 (less than 1% of all measurements). Both stations reveal a significant control of discharge on *LOI*. Negative rating exponents of -0.51 ± 0.03 and -0.47 ± 0.01, for the rivers Rhine and Moselle, respectively, indicate declining organic matter concentrations with increasing discharge. At the Moselle, declining trends are partially explained by seasonal effects, with low discharges and high *LOI* dominating in summer and high discharges and low *LOI* dominating in winter months (Fig. 8 and Fig. 9). However, along the Rhine, seasonal trends are much less pronounced, and *LOI*-values scatter much stronger around the regression line in Fig. 8e+f compared to those of the River Moselle.

Negative rating exponents of *LOI* indicate that suspended matter at low flow is enriched in organic carbon, highlighting the primary control of low flow dynamics with increased water and plankton residence time on *LOI*. In addition to the controlling flow dynamics, higher *LOI* during spring and summer months show the positive effect of water temperature and light availability on plankton growth (Cloern, 1999), which may dominate the total suspended organic matter in the river Moselle at Koblenz especially during April and May (Fig. 9) (Hardenbicker et al., 2014). Under warm low flow conditions, increasing discharges rapidly dilute autochthonous carbon causing a decline of total suspended sediment as evidenced in early summer 2011, which was characterized by exceptionally low discharge of the Rhine in May and June (Hardenbicker et al., 2016). While SSC_{tot} in the Rhine at Koblenz related negatively with discharge during these low-flow months, a positive correlation prevails during the rest of the year 2011, indicating a shift in the SSC regime as phytoplankton dominates the organic suspended fraction.

At stations where the organic fraction of the SSC adds a substantial share to the total SSC, the rating exponent b_l is negative. For instance, in the Elbe increases of LOI and $Chla$ from upstream to downstream (Hardenbicker et al., 2016) are characterized by a generally decreasing trend of b_l (Fig. 6b). Furthermore, low *LOI*-levels in the upper and middle Rhine are characterized by higher b_l-values (~0.5). Thus our results indicate that the suspended sediment rating at low flows is strongly controlled by intrinsic (within-channel) processes that govern the formation of organic matter within the river channel: organic rich channels are generally characterized by b_l-values close to 0 or < 0, while organic poor channels show typically b_l>0.5.

https://doi.org/10.5194/esurf-2020-3
Preprint. Discussion started: 28 January 2020

4.3 Modelling of the total suspended sediment

The presented data indicate that the observed rating break of total suspended sediment concentration is mainly controlled by the transition from autochthonous production of organic suspended matter at low flows to the allochthones supply of (dominantly mineral) suspended matter during high flows. Our results suggest that SSC_{mrl} and LOI can be modelled separately using a power law rating. If the rating behaviour of $SSC_{mrl} = f(Q/Q_{GM})$ and $LOI = f(Q/Q_{GM})$ is known, the organic and total suspended sediment concentration can be estimated:

$$SSC_{org} = \frac{LOI}{1-LOI} SSC_{mrl}, \qquad SSC_{tot} = \left(\frac{LOI}{1-LOI} + 1\right) SSC_{mrl} \tag{4}$$

Using the bootstrap regression of the LOI-station at the River Moselle, with $SSC_{mrl} = (5.27 \pm 0.14) \times (Q/Q_{gm})^{(1.37\pm0.03)}$ and $LOI = (0.32 \pm 0.004) \times (Q/Q_{gm})^{(-0.47\pm0.01)}$, the modelled SSC_{tot} (Fig. 10) shows the following features: i) at very low discharges ($\sim Q/Q_{gm} < 0.2$), SSC_{tot} typically declines with increasing Q , ii) at higher discharges SSC_{tot} increases with discharge, iii) the gradient of the modelled SSC_{tot}-lines continuously increases with Q and approaches the rating exponent of the mineral SSC-fraction at high Q/Q_{gm}. This model result generally agrees with the measured SSC_{tot}-values. The decrease of the modelled SSC_{org}-values at very low discharges support the notion that the organic fraction of the suspended matter is affected by dilution effects. The dilution effect of the autochthonous organic matter is outpaced by increased (allochthones) supply of organic matter, which leads to increasing SSC_{org} at higher discharges as a result of strong supply of organic rich top soils through surface runoff and soil erosion.

Empirical sediment rating curves show distinct rating breaks at roughly $Q/Q_{gm}\sim$ 1 for most stations. In contrast, suspended sediment rating of the modelled SSC_{tot} based on Eq. 4 changes more gradually i) from negative relations at very low discharges, ii) to slight increases of SSC_{tot} at low to medium (average) discharge and iii) to strong increases of SSC_{tot} with Q/Q_{gm} at high discharges. The gradient of the modelled SSC_{tot} at high discharges approaches the rating exponent of SSC_{mrl}, which is similar to the rating exponent b_h in the high flow domain above the rating break. Assuming that a_h and b_h are mainly controlled by the mineral fraction of the suspended sediment, we argue that the rating of the high flow regime can be used as a first order approximation of the SSC_{mrl} at low flow conditions and that the excess of SSC_{tot} compared to the modelled SSC_{mrl} is primarily explained by the organic fraction of the suspended sediment (compare Fig. 10 and 11). Differences between b_h (i.e. the rating at high discharge) and the rating of SSC_{mrl} may be partially explained by the organic fraction of suspended sediment that is not derived from *in situ* (autochthonous) organic matter, but is supplied from hillslope through the erosion of organic rich top soils.

In case of the river Moselle, our results indicate that SSC_{tot} exceeds SSC_{mrl} by a factor of ~1.5 to 2 at discharges smaller than Q_{GM}. Thus, monitored suspended sediment yields, which are mostly based on estimates of the total SSC, overestimate the mineral fraction of the SSC at low to moderate flows. The frequency analysis of the long-term suspended monitoring data at the Rhine station at Koblenz, which integrates the organic and mineral fraction of the suspended matter, shows roughly 50 % of the total annual suspended load is transport in 10% of the time during floods. Due to the inclusion of the organic matter

https://doi.org/10.5194/esurf-2020-3
Preprint. Discussion started: 28 January 2020

and the resulting overestimation of the (mineral) suspended sediment at low to medium flows, floods are likely to be more important in the transport of the mineral fraction of the suspended load. In the case of a clear rating break, our conceptual model separating the rating at low and high flows due to the shift of the process regime can be used to separate the organic and mineral fraction and give a first order estimate of the autochthonous organic fraction of the total SSC.

In the case of substantial share of the organic SSC to the total SSC, our results suggest that the common practice using a continuous sediment rating results in large errors that can be reduced applying rating relationship including scale breaks.

5. Conclusion

Using more than 750 000 suspended sediment and discharge measurements at 62 gauging stations along 19 waterways in Germany and more than 2000 measurements of the loss on ignition of suspended matter at two stations along the rivers Moselle and Rhine, we performed a detailed rating analysis of suspended matter and its organic content. Our main findings may be summarized as follow:

1. For most studied gauging stations, rating coefficients are not constant over the full discharge range, but there is a distinct break in the sediment rating curve, with specific SSC-Q_w domains above and below this break. Typically the rating break occurs at the geometric mean discharge.
2. The transition of the rating exponent (from b_l to b_h) is likely to be a result of a change of controlling factors of the suspended sediment from intrinsic (within the river system) to extrinsic (outside the river channel but within the catchment) factors. Our results suggest that the formation of organic matter within the river channel is an important control of the rating behaviour at low discharges, while the extrinsic control is related to the supply of suspended sediment due to hillslope erosion, as supported by the relationship between the rating exponent and the fraction of hillslopes steeper than 10% within the contributing catchment area.
3. Based on these findings we developed a conceptual rating model separating the mineral and organic fraction of the suspended matter in the Germany waterways. The model assumes a positive power law rating of the mineral fraction of the SSC with Q and a negative power law rating of the LOI with Q and can be used to model the rating behaviour of the total SSC as frequently measured by suspended monitoring networks. An evaluation of this model using data from other river systems in Europe is in progress.

Acknowledgements.

The data used in this paper are taken from the suspended sediment monitoring network of the German waterways that was established in the 1960ties by the Federal Waterways and Shipping Administration (Wasserstraßen- und

https://doi.org/10.5194/esurf-2020-3
Preprint. Discussion started: 28 January 2020

Schifffahrtsverwaltung des Bundes, WSV). We acknowledge the WSV for maintaining the monitoring network and for water sampling.

References

Aich, V., Zimmermann, A., and Elsenbeer, H.: Quantification and interpretation of suspended-sediment discharge hysteresis patterns: How much data do we need?, Catena, 122, 120-129, 2014.

Asselmann, N.: Fitting and interpretation of sediment rating curves, Journal of Hydrology, 234, 228-248, 2000.

Baartman, J. E. M., Masselink, R., Keesstra, S. D., and Temme, A. J. A. M.: Linking landscape morphological complexity and sediment connectivity, Earth Surface Processes and Landforms, 38, 1457-1471, 2013.

Bracken, L. J., Wainwright, J., Ali, G. A., Tetzlaff, D., Smith, M. W., Reaney, S. M., and Roy, A. G.: Concepts of hydrological connectivity: Research approaches, pathways and future agendas, Earth-Science Reviews, 119, 17-34, 2013.

Cleveland, W. S.: LOWESS: A program for smoothing scatterplots by robust locally weighted regression, The American Statistician, 35, 54, 1981.

Cloern, J. E.: The relative importance of light and nutrient limitation of phytoplankton growth: a simple index of coastal ecosystem sensitivity to nutrient enrichment, Aquatic Ecology, 33, 3-16, 1999.

Cohn, T. A., Caulder, D. L., Gilroy, E. J., Zynjuk, L. D., and Summers, R. M.: The validity of a simple statistical model for estimating fluvial constituent loads: An Empirical study involving nutrient loads entering Chesapeake Bay, Water Resources Research, 28, 2353-2363, 1992.

Diplas, P., Kuhnle, R., Gray, J., Glysson, D., and Edwards, T.: Sediment transport measurements. In: Sedimentation engineering: processes, measurements, modeling, and practice, Marcelo, H. G. (Ed.), American Society of Civil Engineers, 2008.

Ferguson, R. I.: River Loads Underestimated by Rating Curves, Water Resources Research, 22, 74-76, 1986.

Fischer, H.: Zur Steuerung der Trophie großer Flüsse, Korrespondenz Wasserwirtschaft, 8, 225-230, 2015.

Frings, R. M., Gehres, N., Promny, M., Middelkoop, H., Schüttrumpf, H., and Vollmer, S.: Today's sediment budget of the Rhine River channel, focusing on the Upper Rhine Graben and Rhenish Massif, Geomorphology, 204, 573-587, 2014.

Frings, R. M., Hillebrand, G., Gehres, N., Banhold, K., Schriever, S., and Hoffmann, T.: From source to mouth: Basin-scale morphodynamics of the Rhine River, Earth-Science Reviews, 196, 2019.

Fryirs, K.: (Dis)Connectivity in catchment sediment cascades: a fresh look at the sediment delivery problem, Earth Surface Processes and Landforms, 38, 30-46, 2013.

Geider, R. J.: Light and Temperature Dependence of the Carbon to Chlorophyll a Ratio in Microalgae and Cyanobacteria: Implications for Physiology and Growth of Phytoplankton, New Phytologist, 106, 1-34, 1987.

Gray, A. B.: The impact of persistent dynamics on suspended sediment load estimation, Geomorphology, 322, 132-147, 2018.

Habersack, H. and Haimann, M.: Schwebstoffmessungen in Österreich ADCP-Messung - Bericht, 2010.

Hardenbicker, P., Rolinski, S., Weitere, M., and Fischer, H.: Contrasting long-term trends and shifts in phytoplankton dynamics in two large rivers, International Review of Hydrobiology, 99, 287-299, 2014.

Hardenbicker, P., Weitere, M., Ritz, S., Schöll, F., and Fischer, H.: Longitudinal Plankton Dynamics in the Rivers Rhine and Elbe, River Research and Applications, 32, 1264-1278, 2016.

Heckmann, T., Cavalli, M., Cerdan, O., Foerster, S., Javaux, M., Lode, E., Smetanová, A., Vericat, D., and Brardinoni, F.: Indices of sediment connectivity: opportunities, challenges and limitations, Earth-Science Reviews, 187, 77-108, 2018.

Hillebrand, G. and Frings, R.: Von der Quelle zur Mündung: Die Sedimentbilanz des Rheins im Zeitraum 1991 – 2010, Bericht KHR/CHR II-22. Internationale Kommission für die Hydrologie des Rheingebietes, Lelystad. ISBN: 978-90-70980-39- 9, DOI: 10.5675/KHR_22.2017., 2017.

Hillebrand, G., Hardenbicker, P., Fischer, H., Otto, W., and Vollmer, S.: Dynamics of total suspended matter and phytoplankton loads in the river Elbe, Journal of Soils and Sediments, 18, 3104-3113, 2018.

Hoffmann, T.: Sediment residence time and connectivity in non-equilibrium and transient geomorphic systems, Earth-Science Reviews, 150, 609-627, 2015.

Hoffmann, T., Glatzel, S., and Dikau, R.: A carbon storage perspective on alluvial sediment storage in the Rhine catchment, Geomorphology, 108, 127-137, 2009.

Hoffmann, T., Hillebrand, G., and Noack, M.: Uncertainty analysis of settling, consolidation and resuspension of cohesive sediments in the Upper Rhine, International Journal of River Basin Management, 15, 401-411, 2017.

https://doi.org/10.5194/esurf-2020-3
Preprint. Discussion started: 28 January 2020

Horowitz, A. J.: An evaluation of sediment rating curves for estimating suspended sediment concentrations for subsequent flux calculations, Hydrological Processes, 17, 3387-3409, 2003.
Morehead, M. D., Syvitski, J. P., Hutton, E. W. H., and Peckham, S. D.: Modeling the temporal variability in the flux of sediment from ungauged river basins, Global and Planetary Change, 39, 95-110, 2003.
Naden, P. S.: The Fine-Sediment Cascade. In: Sediment cascades: an integrated approach, Burt, T. and Allison, R. (Eds.), Wiley-Blackwell, 2010.
Owens, P. N., Batalla, R. J., Collins, A. J., Gomez, B., Hicks, D. M., Horowitz, A. J., Kondolf, G. M., Marden, M., Page, M. J., Peacock, D. H., Petticrew, E. L., Salomons, W., and Trustrum, N. A.: Fine-grained sediment in river systems: environmental significance and management issues, River Research and Applications, 21, 693-717, 2005.
Partheniades, E.: Chapter 4 - The Hydrodynamic Transport Processes of Cohesive Sediments and Governing Equations. In: Cohesive Sediments in Open Channels, Partheniades, E. (Ed.), Butterworth-Heinemann, Boston, 2009.
Poesen, J.: Soil erosion in the Anthropocene: Research needs, Earth Surface Processes and Landforms, 43, 64-84, 2018.
Poulier, G., Launay, M., Le Bescond, C., Thollet, F., Coquery, M., and Le Coz, J.: Combining flux monitoring and data reconstruction to establish annual budgets of suspended particulate matter, mercury and PCB in the Rhône River from Lake Geneva to the Mediterranean Sea, Science of The Total Environment, 658, 457-473, 2019.
Quiel, K., Becker, A., Kirchesch, V., Schöl, A., and Fischer, H.: Influence of global change on phytoplankton and nutrient cycling in the Elbe River., Regional Environmental Change, 11, 405-421, 2011.
Reid, I. and Frostick, L. E.: Discussion of conceptual models of sediment transport in streams. In: Sediment Transport in Gravel-Bed Rivers, Thorne, C. R., Bathurst, J. C., and Hey, R. D. (Eds.), John Wiley, New York, 1987.
Spreafico, M., Lehmann, C., Jakob, A., and Grasso, A.: Feststoffbeobachtung in der Schweiz. Ein Tätigkeitsgebiet der Landeshydrologie, Bundesamt für Wasser und Geologie, Bern, 2005.
Syvitski, J. P., Morehead, M. D., Bahr, D. B., and Mulder, T.: Estimating fluvial sediment transport: The rating parameters, Water Resources Research, 36, 2747-2760, 2000.
Syvitski, J. P., Vörösmarty, C., Kettner, A., and Green, P.: Impact of Humans on the Flux of Terrestrial Sediment to the Global Coastal Ocean, Science, 308, 376-380, 2005.
Thollet, F., Le Bescond, C., Lagouy, M., Gruat, A., Grisot, G., Le Coz, J., Coquery, M., Lepage, H., Gairoard, S., Gattacceca, J. C., Ambrosi, J.-P., and Radakovitch, O.: Observatoire des Sédiments du Rhône. IRSTEA (Ed.), 2018.
Thorp, J. H. and Delong, M. D.: Dominance of autochthonous autotrophic carbon in food webs of heterotrophic rivers., Oikos, 96, 543-550, 2002.
van Rijn, L.: Sediment Transport, Part II: Suspended load transport, Journal of Hydraulic Engineering, ASCE, no 11., Journal of Hydraulic Engineering, 11, 1613-1641, 1984.
Walling, D. E.: Erosion and sediment yield: a global overview, IAHS Publ., 236, 3-19, 1996.
Walling, D. E., Owens, P. N., Waterfall, B. D., Leeks, G. J. L., and Wass, P. D.: The particle size characteristics of fluvial suspended sediment in the Humber and Tweed catchments, UK, Science of The Total Environment, 251, 205-222, 2000.
Warrick, J. A.: Trend analyses with river sediment rating curves, Hydrological Processes, 29, 936-949, 2015.
Wetzel, R.: Limnology. Lake and River Ecosystems, Elsevier, 2001.
Winterwerp, J. and Van Kesteren, W. G. M.: Introduction to the physics of cohesive sediment in the marine environment, Elsevier, Amsterdam, 2004.
Winterwerp, J. C., Manning, A. J., Martens, C., de Mulder, T., and Vanlede, J.: A heuristic formula for turbulence-induced flocculation of cohesive sediment, Estuarine, Coastal and Shelf Science, 68, 195-207, 2006.
Zuecco, G., Penna, D., Borga, M., and van Meerveld, H. J.: A versatile index to characterize hysteresis between hydrological variables at the runoff event timescale, Hydrological Processes, 30, 1449-1466, 2016.

https://doi.org/10.5194/esurf-2020-3
Preprint. Discussion started: 28 January 2020

Earth Surface Dynamics
Discussions
Open Access
EGU

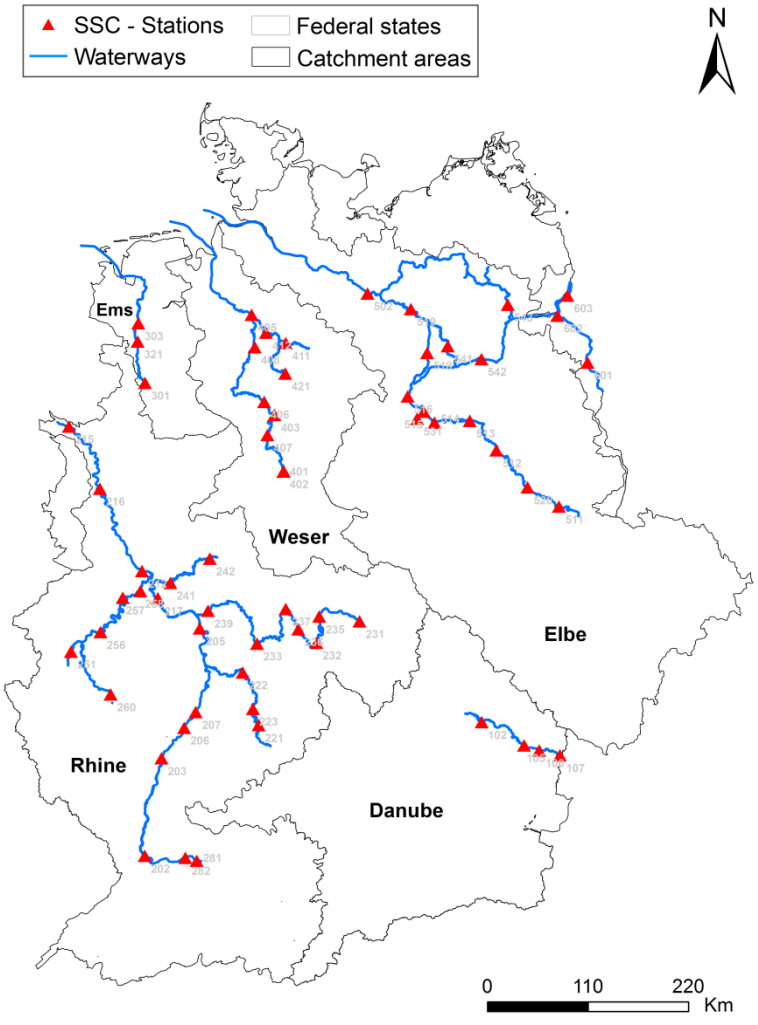

Figure 1: Selected sampling locations of the WSV-suspended monitoring network used in this study. Labels refer to the station codes given in Tab. 1.

https://doi.org/10.5194/esurf-2020-3
Preprint. Discussion started: 28 January 2020

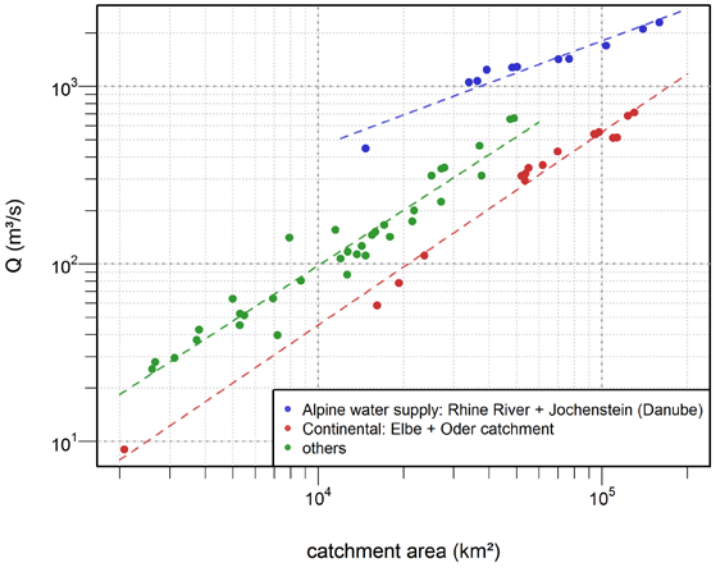

475 **Figure 2: Discharge as a function of catchment area for 62 gauging stations that are used as reference stations of the suspended sediment monitoring network.**

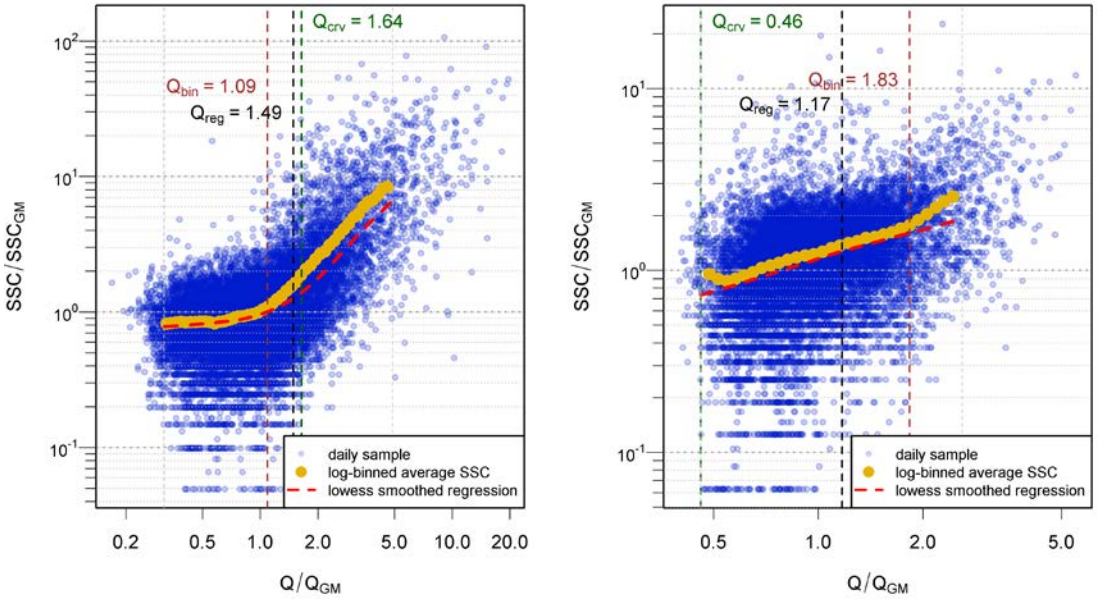

Figure 3: Rating curves of the stations at Rockenau (river Neckar, ID 222) and Kachlet (river Danube, ID 103). For locations see Fig. 1.

480

https://doi.org/10.5194/esurf-2020-3
Preprint. Discussion started: 28 January 2020

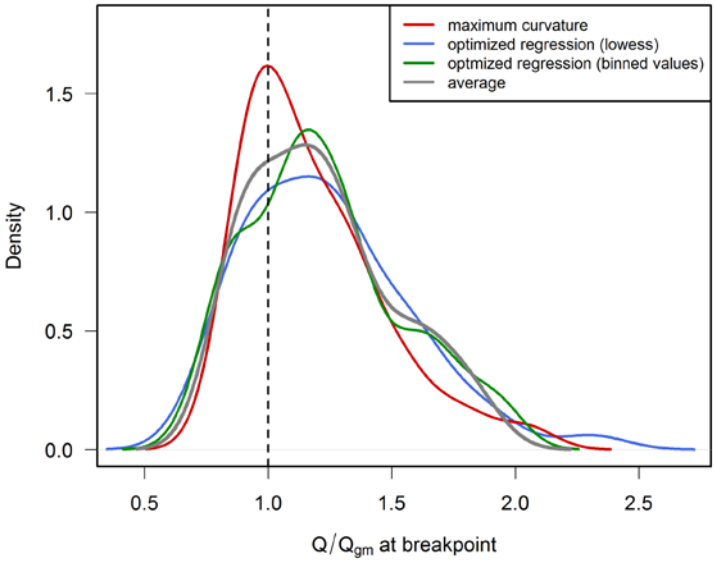

Figure 4: Density distribution of rating breaks (Q_{br}) derived from the scaling analysis of the suspended sediment concentration. For detailed results see also Tab. 2.

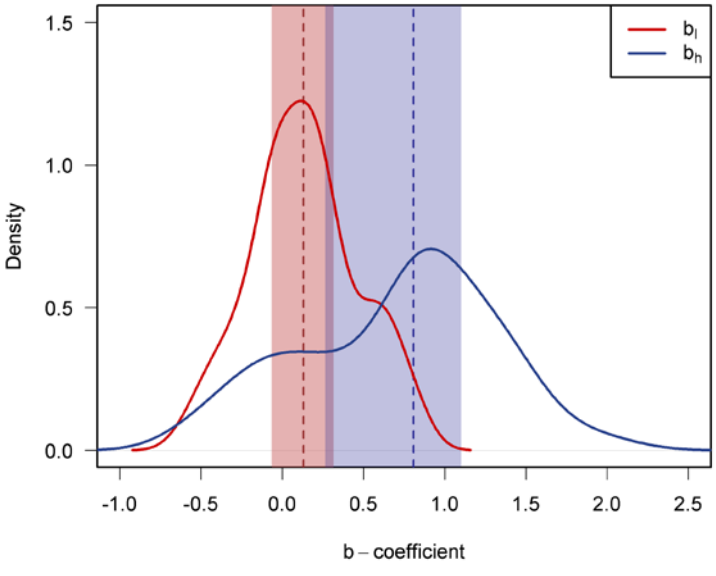

485 **Figure 5: Density distribution of rating exponents (following Eq.2) for the low flow (b_l) and high flow (b_h) regime. The blue and red vertical dashed lines indicate the median values, the blue and red shaded areas indicate the 25% and 75% percentile of both rating coefficients.**

https://doi.org/10.5194/esurf-2020-3
Preprint. Discussion started: 28 January 2020

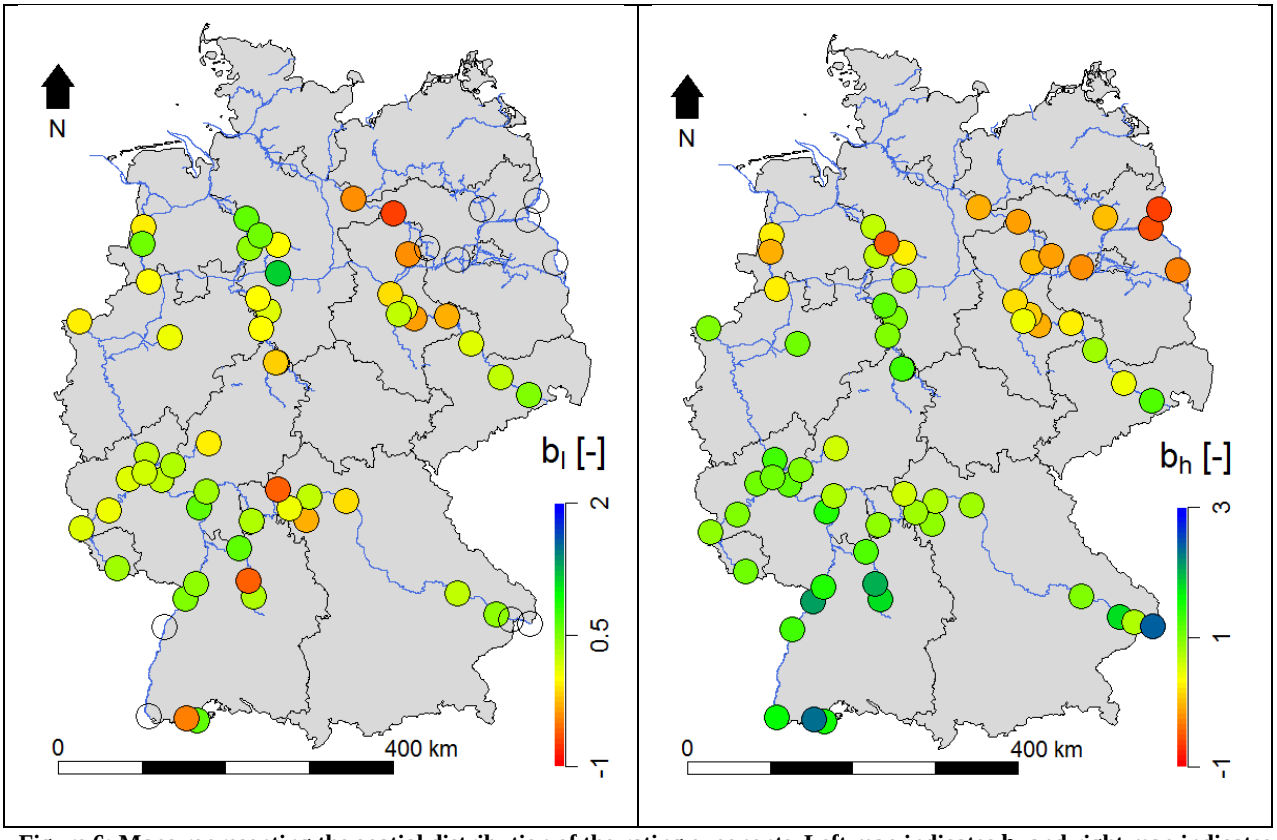

Figure 6: Maps representing the spatial distribution of the rating exponents. Left map indicates b_l and right map indicates b_h.

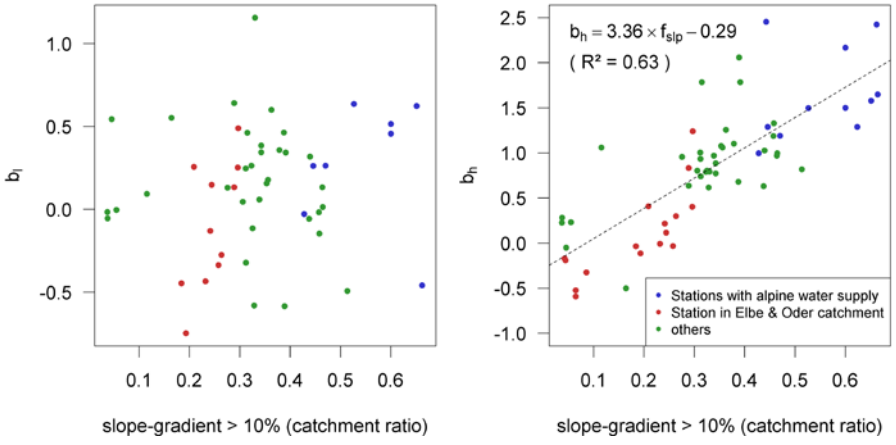

Figure 7: Rating coefficients (b_l left and b_h right) vs ratio of slopes within the contributing catchment with slope gradient steeper 10%.

https://doi.org/10.5194/esurf-2020-3
Preprint. Discussion started: 28 January 2020

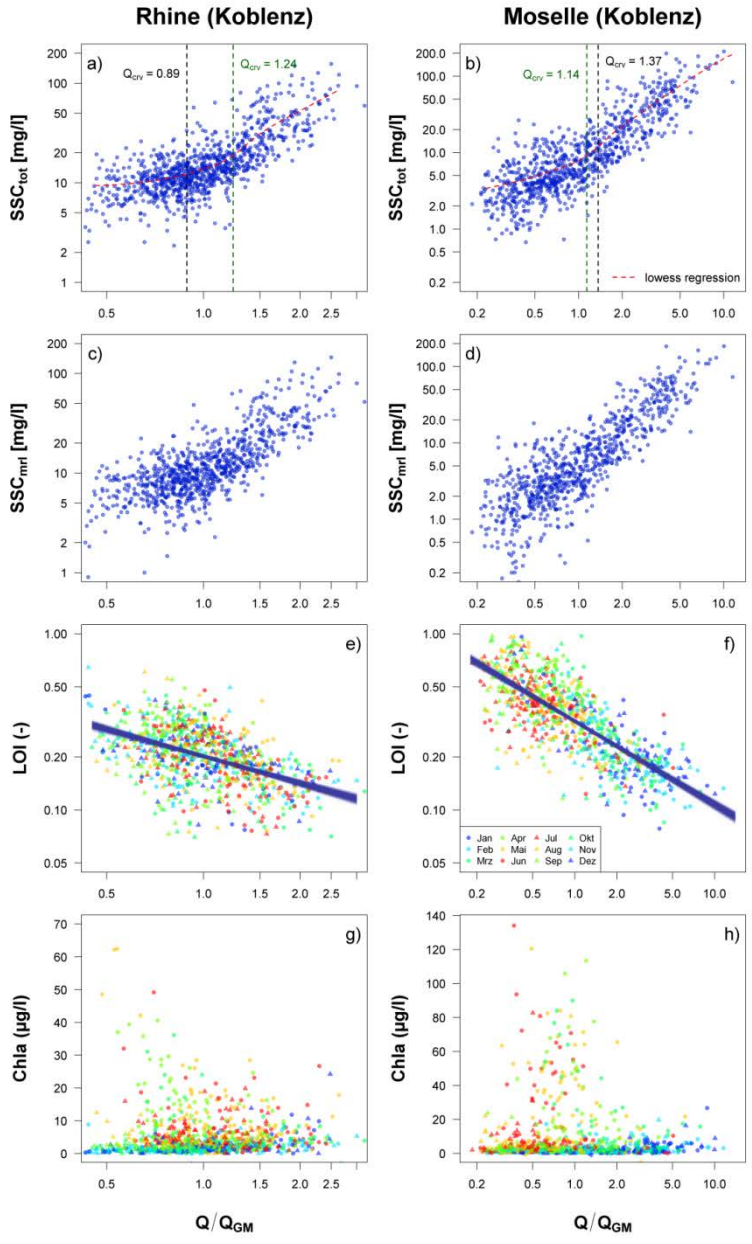

Figure 8: Rating of total SSC (1st line), mineral SSC (2nd line), loss on ignition (LOI, 3rd line) and chlorophyll a (Chla, 4th line) for the station Koblenz-Rhine (left) and Koblenz-Moselle (right). Blue lines on LOI-scatter plots show regression results using 1000 bootstrap-replicates.

https://doi.org/10.5194/esurf-2020-3
Preprint. Discussion started: 28 January 2020

Earth Surface Dynamics Discussions
Open Access
EGU

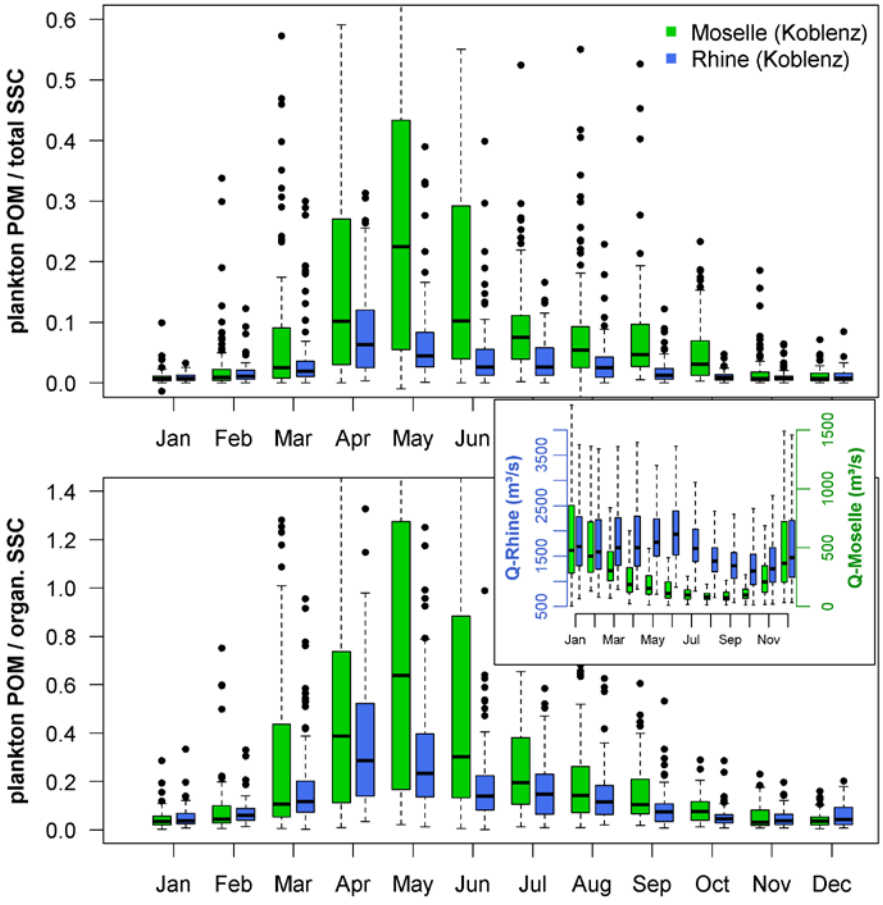

500 **Figure 9: Boxplot of seasonal variation of plankton POM with respect to total *SSC* (top) and organic *SSC* (bottom) for the stations Koblenz Rhine (blue) and Koblenz Moselle (green) from 1990-2017. Organic *SSC* is derived from *LOI* measurements and plankton *POM* is calculated from *Chla*-measurements using a *POC/Chla*-ratio of 40 and a *POC/POM*-ratio of 0.42. Plankton POM/organic SSC ratios > 1 are due to measurement errors of *Chla* and *LOI* and due to simplified conversion ratios. The inset shows the boxplot of seasonal discharge variations at both stations.**

505

https://doi.org/10.5194/esurf-2020-3
Preprint. Discussion started: 28 January 2020

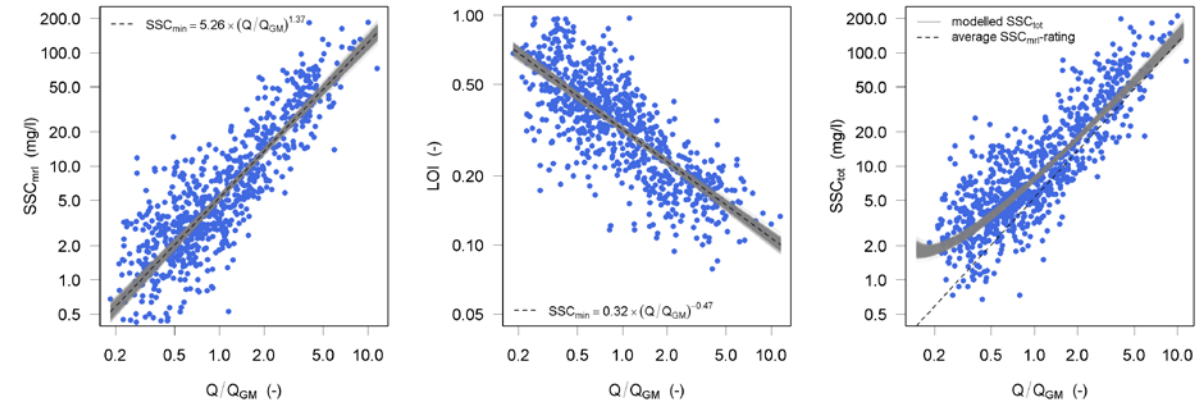

Figure 10: Statistical modelling of the total suspended sediment concentration (*SSC$_{tot}$*, right) based on the positive and negative power law rating of the mineral fraction of the SSC (*SSC$_{mrl}$*, left) and the loss on ignition (*LOI*, middle), respectively.

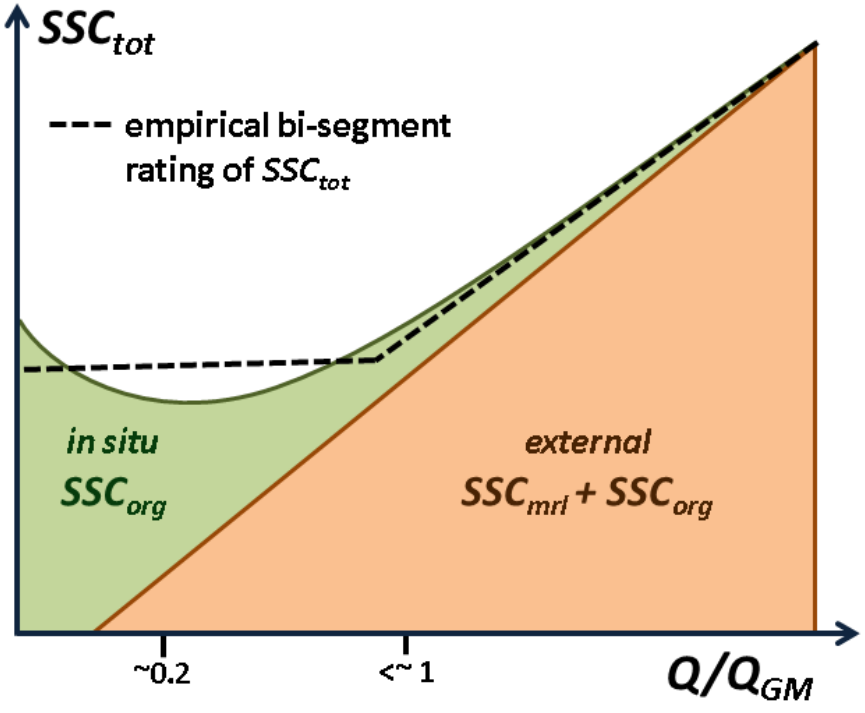

Figure 11: Conceptual model of suspended sediment rating in the German waterways.

https://doi.org/10.5194/esurf-2020-3
Preprint. Discussion started: 28 January 2020

Earth Surface Dynamics Discussions
Open Access
EGU

Table 1: Overview of sampling locations, contributing catchment size, monitoring period, number of samples (n) and average (avg), median (med) and geometric mean (GM) of discharge Q and suspended sediment concentration (SSC). The map index refers to the numbers in the map (Figure 1).

Map index	Station name	River	Location (river-km)	Catchment (km²)	Monitoring period	n	Q (mg/l)			SSC (mg/l)		
							avg	med	GM	avg	med	GM
102	Straubing	Donau	2321,3	37026	1982	7197	462	395	414	16,9	14	13,5
105	Vilshofen	Donau	2249,5	47609	1966	11282	651	573	597	20,0	16	15,3
106	Kachlet	Donau	2230,7	49045	1975	9214	661	578	606	20,4	17	16,1
107	Jochenstein	Donau	2203,1	76653	1974	9174	1425	1292	1319	47,9	23	25,2
281	Reckingen	Rhein	90,2	14718	1972	10038	446	411	416	13,9	10	10,6
282	Albbruck Dogern	Rhein	108,9	33987	1972	10601	1053	969	974	19,7	13	13,0
202	Weil	Rhein	173	36472	1970	10104	1070	984	985	27,5	17	17,0
203	Kehl	Rhein	294	39330	1970-2013	11201	1237	1134	1145	16,4	11	11,4
206	Plittersdorf	Rhein	339,8	48276	1977-2013	9281	1278	1170	1187	18,3	14	14,2
207	Maxau	Rhein	362,3	50196	1964	13203	1285	1175	1189	22,9	18	16,8
205	Nierstein	Rhein	480,6	70387	1983	7228	1419	1283	1315	21,1	17	17,1
217	Sankt Goar	Rhein	557	103488	1970	11398	1694	1520	1557	26,3	21	20,3
215	Emmerich	Rhein	851,9	159555	1982	8710	2289	1950	2072	27,2	25	22,7
212	Weißenthurm	Rhein	608,2	139549	1971	9919	2102	1830	1893	32,9	25	25,9
221	Poppenweiler	Neckar	164,9	5005	1965-2014	11609	64	45	49	30,7	18	17,5
222	Rockenau	Neckar	61,3	7916	1971	10364	140	104	109	34,7	19	20,3
223	Lauffen	Neckar	125,1	12676	1987	6209	87	65	69	22,0	15	14,8
231	Viereth	Main	380,8	12010	1972-2005	8455	107	78	86	18,6	16	15,2
235	Garstadt	Main	323,7	12722	1986-2005	4949	117	82	93	23,4	19	18,7
232	Marktbreit	Main	275,7	13693	1965-2012	11801	113	83	91	25,8	21	19,5
236	Erlabrunn	Main	241,2	14244	1986-2005	4941	126	90	101	25,3	21	20,9
237	Steinbach	Main	210	17914	1987	6121	142	103	114	20,3	17	16,2
233	Kleinheubach	Main	121,7	21505	1973-2014	9702	173	124	136	27,6	22	21,0
239	Eddersheim	Main	15,6	27100	1986-2012	6506	223	161	177	28,9	23	22,8
242	Wetzlar	Lahn	125,3	2669	1986-2007	4843	28	16	18	20,9	17	15,9
241	Kalkofen	Lahn	31,6	5303	1970	10240	45	26	30	22,2	14	13,4
277	Hamm. Wehr	Lippe	120,1	2607	1976	8737	26	19	20	15,6	12	11,7
260	Güdingen	Saar	91,7	3811	1973	10314	42	26	29	18,3	11	10,7
251	Wincheringen	Mosel	221,9	11522	1974	9558	155	91	99	31,7	22	23,2
256	Detzem	Mosel	166,8	25130	1981-2002	5320	314	183	205	31,7	21	22,3
257	Cochem	Mosel	50,2	27165	1981-2011	7387	343	211	231	29,4	19	21,5
258	Brodenbach	Mosel	27,2	27872	1981-2009	6672	349	214	235	31,9	21	22,4
321	Meppen	Hase	1	3126	1974-1996	5740	29	22	24	21,9	21	19,4

https://doi.org/10.5194/esurf-2020-3
Preprint. Discussion started: 28 January 2020

301	Rheine	Ems	153	3740	1964	13506	37	23	25	27,4	18	17,4
303	Lathen	Ems	253,3	8696	1966	12951	80	57	61	18,6	16	14,6
421	Herrenhausen	Leine	87,1	5304	1965-2006	10448	52	38	41	40,0	24	23,8
411	Marklendorf	Aller	75,9	7209	1971	11563	40	30	32	14,9	14	12,5
412	Rethem	Aller	34,2	14730	1973	10601	111	85	91	21,4	19	17,6
401	Hann.-Münden.W.	Werra	0,5	5497	1965	12639	51	38	40	51,6	39	39,0
402	Hann.-Münden.F.	Fulda	1	6947	1965	12639	64	43	51	23,3	18	16,0
407	Höxter	Weser	69,4	15501	1983	8224	145	103	118	30,4	23	23,0
403	Bodenwerder	Weser	110,7	15924	1964	12875	151	109	123	32,3	24	23,7
406	Hameln	Weser	135,2	17077	1979	9333	166	118	134	32,0	24	23,6
408	Nienburg	Weser	268,1	21815	1985	7862	199	143	163	29,5	23	22,7
405	Intschede	Weser	329,5	37720	1969	11270	313	234	256	35,1	28	27,3
543	Zehdenick	Havel	15,1	2076	1991	4290	9	7,5	7,1	10,7	9	8,7
542	Ketzin	Havel	34,1	16173	1991-2016	6310	58	54	45	12,9	11	9,8
541	Rathenow	Havel	103,6	19288	1991-2016	6498	78	72	64	14,9	13	11,8
531	Calbe	Saale	20	23719	1991	6740	111	84	93	26,8	20	21,7
511	Pirna	Elbe	34,7	52080	1991	6120	313	234	257	22,7	18	16,8
520	Meissen	Elbe	83,4	53885	1994	5310	323	239	264	25,1	19	19,8
512	Torgau	Elbe	154	55211	1993	5790	346	253	282	32,1	27	26,1
513	Wittenberg	Elbe	216,3	61879	1991	6339	360	272	295	28,0	24	23,8
514	Aken	Elbe	274,8	69849	1991	5887	429	326	353	25,3	23	21,8
515	Barby	Elbe	294,8	94060	1991	6431	538	401	447	33,1	28	27,9
516	Magdeburg Strombr.	Elbe	326,6	94942	1992	6395	537	397	447	26,0	21	20,8
518	Tangermünde	Elbe	389,1	97780	1991	6397	552	422	462	31,2	27	26,3
519	Wittenberge	Elbe	454,6	123532	1993	5907	681	526	576	32,0	25	26,1
502	Hitzacker	Elbe	522,6	129877	1963	13703	712	571	605	34,0	30	28,4
601	Frankfurt / Oder	Oder	585,8	53590	1991	4822	294	246	252	24,8	21	20,6
602	Hohensaaten	Oder	662,3	109564	1991	4943	512	440	453	21,7	18	17,6
603	Schwedt	Oder	690,6	112950	1991	5022	513	442	454	23,8	20	19,4

https://doi.org/10.5194/esurf-2020-3
Preprint. Discussion started: 28 January 2020

Earth Surface Dynamics Discussions
Open Access
EGU

520 **Table 2: Results from rating-break analysis and and log-linear and non-linear least square regression of rating exponent (Eq. 2) above (b_h) and below (b_l) rating break (Q_{br}/Q_{gm}).**

Map index	name	Q_{br}/Q_{gm}				log-linear regression				non-linear LS regression			
		loess-regression	loess-curvature	binned regression	mean	b_l	Δb_l	b_h	Δb_h	b_l	Δb_l	b_h	Δb_h
102	Straubing	1,03	1,09	1,09	1,07	0,28	0,04	0,97	0,04	0,25	0,08	1,01	0,08
105	Vilshofen	1,55	1,55	1,54	1,55	0,65	0,03	1,50	0,07	0,46	0,07	1,79	0,11
106	Kachlet	-	-	-	-	-	-	0,68	0,02	-	-	0,74	0,03
107	Jochenstein	-	-	-	-	-	-	2,01	0,02	-	-	2,45	0,15
202	Weil	-	-	-	-	-	-	1,23	0,02	-	-	1,65	0,22
203	Kehl	-	-	-	-	-	-	0,85	0,02	-	-	1,29	0,08
205	Nierstein	1,09	1,05	1,15	1,1	0,65	0,04	1,44	0,04	0,64	0,07	1,50	0,09
206	Plittersdorf	1,31	1,29	1,37	1,32	0,69	0,04	1,80	0,07	0,52	0,09	2,17	0,15
207	Maxau	0,95	0,97	0,87	0,93	0,60	0,04	1,41	0,03	0,46	0,06	1,50	0,05
212	Weißenthurm	0,95	0,99	0,87	0,94	0,36	0,03	1,18	0,03	0,26	0,07	1,29	0,05
215	Emmerich	1,08	1,11	1,15	1,11	-0,02	0,04	0,93	0,04	-0,03	0,05	1,00	0,05
217	Sankt Goar	1,01	1,01	1,03	1,02	0,21	0,04	1,22	0,03	0,26	0,06	1,19	0,06
221	Poppenweiler	1,61	1,72	1,83	1,72	0,23	0,02	1,52	0,05	0,34	0,12	1,79	0,08
222	Rocke-u	-	-	1,09	1,09	0,15	0,02	1,37	0,03	0,60	0,09	1,26	0,05
223	Lauffen	1,33	1,39	1,63	1,45	0,12	0,03	1,31	0,06	-0,59	0,19	2,06	0,13
231	Viereth	1,28	1,15	1,09	1,17	-0,01	0,03	0,70	0,03	-0,11	0,10	0,80	0,09
232	Marktbreit	1,01	1,02	1,09	1,04	-0,26	0,03	0,87	0,03	-0,32	0,05	0,94	0,05
233	Kleinheubach	1,17	1,12	1,3	1,2	0,25	0,03	0,92	0,03	0,35	0,04	0,89	0,04
235	Garstadt	1,27	-	1,3	1,29	0,25	0,04	0,74	0,04	0,26	0,06	0,79	0,06
236	Erlabrunn	1,19	-	1,3	1,25	0,13	0,03	0,70	0,04	0,05	0,06	0,80	0,06
237	Steinbach	0,79	0,84	0,82	0,82	-0,43	0,05	0,50	0,03	-0,58	0,08	0,62	0,06
239	Eddersheim	1,44	1,41	1,15	1,33	0,34	0,03	0,77	0,04	0,39	0,05	0,77	0,05
241	Kalkofen	1,94	1,83	1,54	1,77	-0,11	0,03	1,34	0,04	0,32	0,05	1,03	0,05
242	Wetzlar	1,64	1,19	1,37	1,4	-0,25	0,03	0,72	0,03	-0,06	0,04	0,63	0,04
251	Wincheringen	1,35	-	1,3	1,33	0,01	0,01	1,05	0,02	0,13	0,03	0,96	0,02
256	Detzem	1,19	-	1,03	1,11	-0,08	0,02	0,98	0,03	0,06	0,05	0,97	0,04
257	Cochem	1,19	1,31	1,22	1,24	0,18	0,02	1,01	0,02	0,16	0,05	1,08	0,04
258	Brodenbach	1,27	1,37	1,22	1,29	0,17	0,02	1,00	0,03	0,18	0,05	1,06	0,05
260	Güdingen	2,31	2,05	1,15	1,84	0,29	0,03	0,74	0,06	0,36	0,24	1,10	0,21
277	Hamm. Wehr	1,33	1,32	1,37	1,34	0,07	0,02	1,07	0,03	0,09	0,04	1,06	0,05
281	Reckingen	1,15	-	-	1,15	0,81	0,04	0,96	0,06	0,62	0,12	1,58	0,18
	Albbruck	-	-	0,87	0,87								
282	Dogern					0,80	0,05	1,40	0,04	-0,46	0,39	2,42	0,27
301	Rheine	1,3	1,05	1,15	1,17	-0,05	0,02	0,26	0,03	-0,02	0,04	0,23	0,03

https://doi.org/10.5194/esurf-2020-3
Preprint. Discussion started: 28 January 2020

Earth Surface Dynamics Discussions
Open Access
EGU

303	Lathen	0,8	0,91	0,87	0,86	-0,11	0,03	0,27	0,02	-0,05	0,02	0,28	0,02
321	Meppen	1,14	-	1,15	1,15	0,61	0,02	-0,11	0,03	0,54	0,03	-0,05	0,03
401	Hann.-Münden.W.	1,18	1,18	1,09	1,15	-0,46	0,02	0,77	0,03	-0,49	0,06	0,82	0,06
402	Hann.-Münden.F.	1,54	1,29	1,94	1,59	-0,06	0,03	1,11	0,05	-0,15	0,09	1,33	0,11
403	Bodenwerder	1,61	-	1,63	1,62	0,08	0,03	0,83	0,05	0,13	0,06	0,97	0,08
405	Intschede	-	-	1,22	1,22	0,49	0,02	0,70	0,03	0,64	0,03	0,64	0,03
406	Hameln	1,84	1,56	1,73	1,71	-0,07	0,03	1,17	0,05	-0,02	0,06	1,19	0,08
407	Höxter	1,33	1,28	1,3	1,3	-0,06	0,03	0,95	0,04	0,01	0,07	1,00	0,07
408	Nienburg	1,62	1,52	1,73	1,62	0,31	0,03	0,79	0,05	0,46	0,04	0,68	0,05
411	Marklendorf	0,76	0,99	0,73	0,83	0,00	0,03	0,31	0,02	0,00	0,03	0,23	0,01
412	Rethem	1,51	-	1,63	1,57	0,52	0,02	-0,44	0,03	0,55	0,03	-0,50	0,04
421	Herrenhausen	0,92	1,21	0,77	0,97	0,54	0,03	0,88	0,03	1,16	0,06	0,79	0,03
502	Hitzacker	1,26	1,08	1,3	1,21	-0,41	0,02	-0,06	0,03	-0,45	0,02	-0,03	0,03
511	Pir-	1,8	-	1,94	1,87	0,40	0,03	1,39	0,07	0,49	0,06	1,24	0,11
512	Torgau	1,46	-	1,45	1,46	0,15	0,03	0,86	0,04	0,13	0,04	0,83	0,05
513	Wittenberg	0,87	0,91	0,87	0,88	-0,16	0,04	0,26	0,02	-0,28	0,04	0,30	0,02
514	Aken	0,92	0,93	0,82	0,89	-0,25	0,04	-0,04	0,03	-0,34	0,04	-0,03	0,03
515	Barby	0,92	0,88	0,87	0,89	0,13	0,04	0,08	0,03	0,15	0,05	0,12	0,02
516	Magdeburg Strombr.	0,97	0,97	-	0,97	-0,04	0,05	0,19	0,03	-0,13	0,04	0,22	0,03
518	Tangermünde	0,93	0,91	0,92	0,92	-0,28	0,04	-0,06	0,02	-0,43	0,04	-0,01	0,03
519	Wittenberge	1,04	0,94	1,03	1	-0,57	0,04	-0,14	0,03	-0,75	0,04	-0,11	0,03
520	Meissen	0,78	0,86	-	0,82	0,21	0,05	0,36	0,03	0,25	0,06	0,40	0,04
531	Calbe	0,87	0,92	-	0,9	0,11	0,04	0,32	0,03	0,26	0,06	0,41	0,04
541	Rathenow	-	-	-	-	-	-	-0,22	0,01	-	-	-0,17	0,01
542	Ketzin	-	-	-	-	-	-	-0,22	0,01	-	-	-0,19	0,01
543	Zehdenick	-	-	-	-	-	-	0,04	0,01	-	-	0,04	0,02
601	Frankfurt / Oder	-	-	-	-	-	-	-0,24	0,02	-	-	-0,33	0,02
602	Hohensaaten	-	-	-	-	-	-	-0,49	0,02	-	-	-0,52	0,02
603	Schwedt	-	-	-	-	-	-	-0,53	0,02	-	-	-0,59	0,02
999	Koblenz (Rhein)	0.96	0.97		0.96					0,29	0,20	2,26	0,18
998	Koblenz (Mosel)	0.87	0.94		0.91					-0,03	0,07	1,54	0,14